MINERALOGICAL CHARACTERIZATION OF THE GLAUCONITIC SANDSTONE FROM CHICHALI FORMATION OF SURGHAR RANGE

M S Akhtar [a]* and D A Jenkins [b]

[a]*National Agricultural Research Centre, Islamabad, Pakistan*

[b]*School of Agriculture and Forest Sciences, University College of North Wales Bangor, Gwynedd, UK*

Detailed mineralogical characteristics of the Chichali Formation glauconitic sandstone, as a possible source of K for crop production, were determined. It contained 66.8% sand (+50 µm), 19.6% silt (2-50 µm), 9.8% clay (<2 µm) size fractions. The sand and silt fractions were composed of dominantly quartz and mica. As determined by the total K analysis, the sand had 31% mica and the silt had 55%. Mica in the clay was about 52% as indicated by total K content. Also, the clay had 4% vermiculite and 11% smectite. Most clay particles were platy with difused boundaries. The interlayer space had a repeat distance of 10.2 Å as seen under the TEM at high resolution. The study suggests that clay fraction is a disordered glauconite. The presence of about 25% kaolinite indicates the K-deficient geo-chemical environment toward end of the glauconitization process.

Key words: Glauconitic sand stone, Minerological characterization, K content.

Introduction

Glauconitic sandstone is found in the Chichali Formation of Surghar range at approximately Latitude 32°45' N and Longitude 71°25' E (Baqri *et al* 1994). Geologically, Surghar range is a member of Trans-Indus Mountains in the Punjab province of Pakistan. Chichali consists of predominantly dark-greenish-gray glauconitic sandstone with gray calcareous claystone in the lower part and sand-sized glauconite grains cemented with $CaCO_3$ in the middle. It is about 70 M thick and has cropped out as friable or loosely coherent glauconitic sandstone (Denilchik and Shah 1987). Age of the Chichali Formation is late Jurassic to early Cretaceous (Fatmi 1972). Based on petrographic observation and whole rock powder X-ray diffraction, some generalized mineralogy of a near by gluconitic sandstone (Kussak Formation, Khewra Gorge, Salt Range) was presented previously (Baqri 1994). Yet, detailed characterization of mineral contained in different size fractions at high resolution is needed to understand K-release behaviour, while such information is scanty.

Mineralogically, glauconite is true dioctahedral mica with Fe^{+3} substituted for Al in the octahedral sheet and contains less K than the other true K containing mica, e.g., muscovite. Interstratification with expandable layer is present in varying degrees (Bailey 1980). An ordered gluconite, with < 10% expandable layers, contains at least 7.0 wt % K_2O (Birch *et al* 1976). Potassium content of glauconite, as in case of illite, is directly related to the content of non-expandable layers in

the structure; increasing non-expandable portion increases K_2O contents (Brindley 1980). Glauconite has higher 001/003 intensity ratio than illite but very weak or non-existent 002 reflection. Heavy scattering from octahedral iron (Moore and Reynold 1989) causes lower intensity of 002 reflection.

Locally, the glauconitic sandstone is called "Greensand" and is known to have fertilizer value among the local farming community. Objective of this paper is to report mineralogical characteristics of this sandstone as possible source of K for crop production.

Materials and Methods

The original sample was crushed gently in acetone and the powder was dispersed in pH 9.5 Na_2CO_3. The suspension was fractionated into sand (+ 50 µm), silt (50-2 µm), and clay (< 2 µm) fractions without any chemical pretreatment. The sand and silt fractions were oven dried while the clay was freeze dried. Randomly oriented powder mounts of the silt and sand-powder were X-rayed. Also, mineral composition of the clay was determined using preferentially oriented mounts of the Mg and K-saturated clay. After initial X-ray analysis, the Mg-saturated clay was glycerol solvated and X-rayed again, while K-saturated clay was heat-treated to 623 Kelvin and 823 Kelvin in two steps and X-rayed after each heat treatment.

For the differential thermal analysis (DTA), total chemical analysis, cation exchange capacity (CEC) and scanning and transmission electron microscopy, the sand, silt and clay size

*Author for correspondence. E.mail: msa@lrri. Sdnpk.undp.org.

fractions were treated with H_2O_2 to remove organic matter. For DTA the 100 mg each of sand, silt, and clay were packed in the ceramic cup and heated from 293 Kelvin to 1273 Kelvin at the rate of 10 Kelvin per minute using a PtRh/Pt thermocouple on a Netzsch 410 DTA equipment.

For Transmission Electron Microscope (TEM) the clay was mounted on carbon coated gold grids and viewed with a JEOL KX100 instrument operated at 80 kV. For morphological characterization, the sand and silt fractions were suspended in acetone and mounted on aluminum stub. After sputtered coating with gold, the specimens were viewed under a JEOL 35 scanning electron microscope (SEM) operated at 15 kV.

Hand specimen was impregnated using epoxy resin (Inn and Pluth 1970) to study the spatial distribution and morphology of particle *in situ*. Thin section was viewed under both light and scanning microscope. Further, each size fraction was dissolved in HF-aqua regia and total elements were determined by Perkenalmer 400 atomic absorption. Mica in various size fractions was calculated from K content assuming 10% K_2O in the sand and silt fractions and 7% K_2O in the clay fraction (Birch *et al* 1976). Vermiculite and smectite content in the clay fraction was determined with Ca/Mg and K/NH_4 cation exchange capacity method (Jackson 1979).

Maize (*Zea mays*) seedlings were grown for 6 weeks to see K availability over plant growth period, with and without-K and with 10 g of the crushed glauconitic sandstone added to

nutrient solution. Plant shoot and root dry weight was recorded and plant K concentration was determined by digesting the material in perchloric acid. Potassium released in the nutrient solution and digested plant was assayed by flamephotometer.

Results and Discussion

Sand and silt fractions. Sand size particles of round to angular blocky shape with sharp edges and rough, fractured surface (Fig 1A, B) make up bulk of the glauconitic sediment (Table 1). Large sand matrix with 3 % of organic matter by weight and water contents contributes to its friable nature. Presence of organic matter was confirmed by DTA exothermic peak (data not presented). The clay size particles were oriented parallel to the skeleton particles (Fig 1F, G). The sand surfaces showed signs of deep etching either due to dissolution or re-precipitation. On the other hand, the silt fraction, which was 20%, had irregular to rhombohedral shape grains with clean smooth surfaces (Fig 1C, D). Many silt particles exhibited layered structure indicative of phyllosilicate morphology (Fig 1E). The layered particles had thin frayed edges.

The sand and silt fractions of the sediment contained mainly quartz and mica as determined by X-ray diffraction (data not presented). The mica content in the sand and silt as indicated by the XRD peak intensity appeared to be lesser than that determined by chemical analysis. The low XRD peak intensity was due to random orientation of the particles in the

Table 1
Particle size distribution, quantitative mineralogy and total elemental analysis of the separates

Particle size distribution

Size fraction	%
Sand (+ 50 µm)	67
Silt (50-2 µm)	20
Clay (< 2 µm)	10

Mineralogy	Glauconitic Sandstone		@Glauconite	Hectorite	
	+ 50 µm	50-2 µm	< 2 µm	Whole	< 2 µm
			.....(%).....		
Mica	31	55	52	57	1
Vermiculite	-	-	4	10	3
Smectite	-	-	11	6	92
Total elemental analysis			.....mmol $(100g)^{-1}$.....		
Potassium*	65	116	77	85	3
Iron	191	286	188	123	0
Magnesium	31	51	34	41	823

@, Glauconite from the South end of the football stadium Madison, Wisconsin; #, Hectorite Hector California, Ex. Wards Natural Science Establishment.
*, The conversion factors to change K, Fe, and Mg mmol 100 g^{-1} to $K_2O\%$, $Fe_2O_3\%$, and $MgO\%$, respectively, are 0.0459, 0.08, and 0.0403.
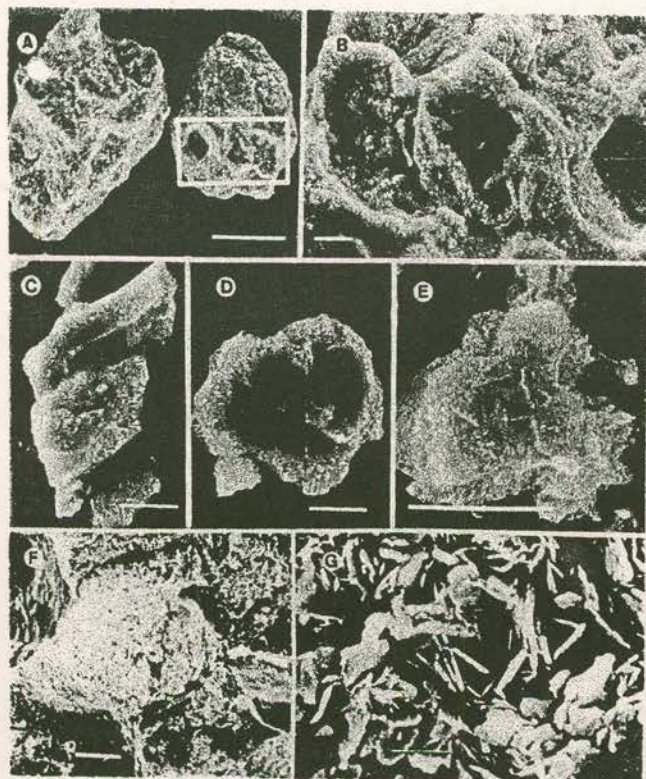
Fig 1. Scanning electron microscope (SEM) micrographs of the sand and silt fractions: (A) blocky and spheroidal particles with sharp edges and fractured surface, (B) magnified view of selected area from 'A' showing signs of surface precipitation, bottom of the pits show original surfaces of the grain, (C) rhombohedral particle with clean surface and sharp edges; (D) spheroidal particle with clean surface and rounded edges; (E) layered particle with frayed edges curling upword; (F) SEM micrograph of thin section showing *in situ* distribution of clay and (G) glauconitic platy particles occurring perpendicular to the skeleton grains.

Bar = 50 μm in A, B, and F and 5 μm in C, D, E and G.

Table 2
Biomass production, solution K, and plant K

Treatment	Shoot-wt	Root-wt	Solution-K	Plant-K
	(g pot^{-1})		(mg kg^{-1})	
-K	0.7	0.2	0.0	2600
Glauconite	2.5	0.8	0.1	4000
+ K	5.8	2.1	19.5	8000

powder mounts as well as low crystallinity. Also, the second order (002) peak was almost nonexistent which is due to high scattering of X-rays by octahedral Fe. The sand contained lower mica than the silt fraction as determined by the total K analysis (Table 1). The relative distribution of Fe and Mg suggested that mica contained in the sand and silt is probably glauconitic in nature. The extra amount of Fe may have been contributed by goethite.
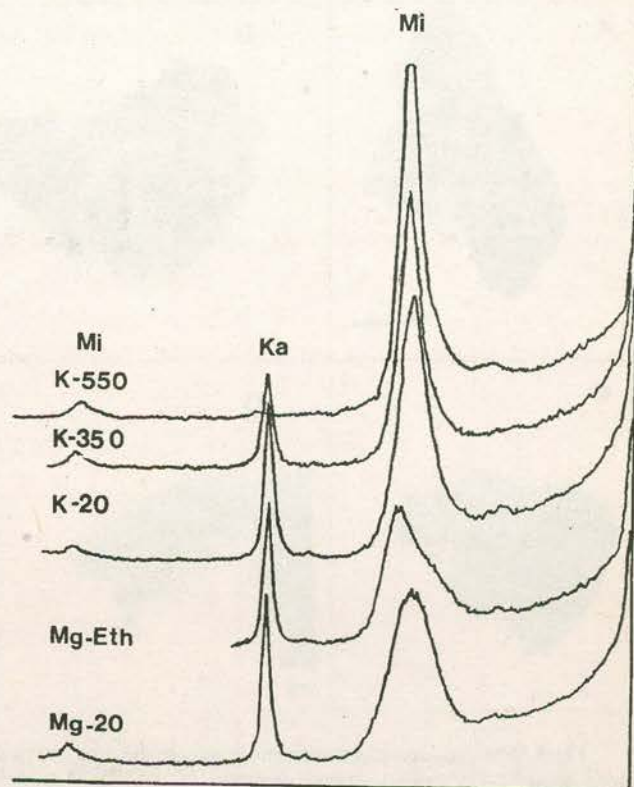

Fig 2. X-ray diffraction pattern of the clay (< 2 μm size fraction.

Preparative treatments for XRD analyses are abbreviated as: Mg-Eth, Mg-saturated and glycerated; Mg-25, Mg-saturated at 298K; K-25, K-350, and K-550, K-saturated at 298K and heat treated for two hours at 623 and 823K, respectively: Mi, mica; Ka, kaolinite.
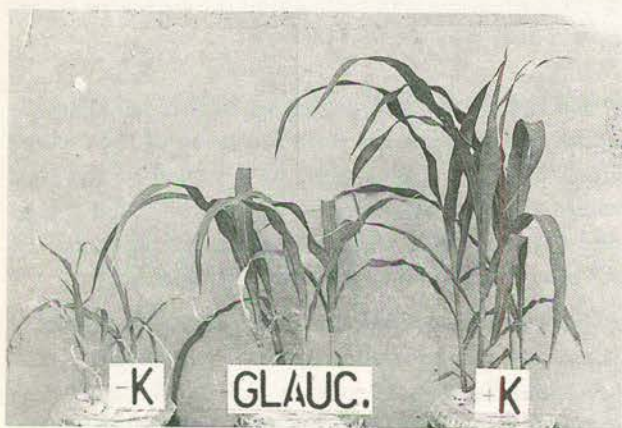
The sand and silt fractions had greater Fe/Mg ratio than the reference glauconite (taken from south end of the football stadium, Madison, Wisconsin). As revealed by the total elemental analysis, the sand fraction had 190 mmol 100 g^{-1} Fe and 30 mmol 100 g^{-1} Mg whereas the silt contained 290 mmol 100 g^{-1} Fe and 50 mmol 100 g^{-1} Mg (Table 1).

Clay fraction. Xray diffraction data indicated a mixture of mica and kaolinite minerals in the clay fraction (Fig 2) The Mg-saturated clay showed peaks at 10.3, 7.0, 5.0, and 3.33Å Å indicating the presence of mica and kaolinite. The glycerol solvation of Mg-saturated clay upon did not affect the XRD pattern except that the 10.3 Å peak was broadened at the base resulting in a shoulder on lower angle side of the basal reflection. This broadening of peak indicated the presence of smectite, which had expanded to various degrees resulting in a broad diffraction peak. By visual comparison with Thompson and Hower (1975) X-ray diffraction data, it was estimated that the glauconite contained about 10% expandable layers. This observation was further supported by the CEC determina-
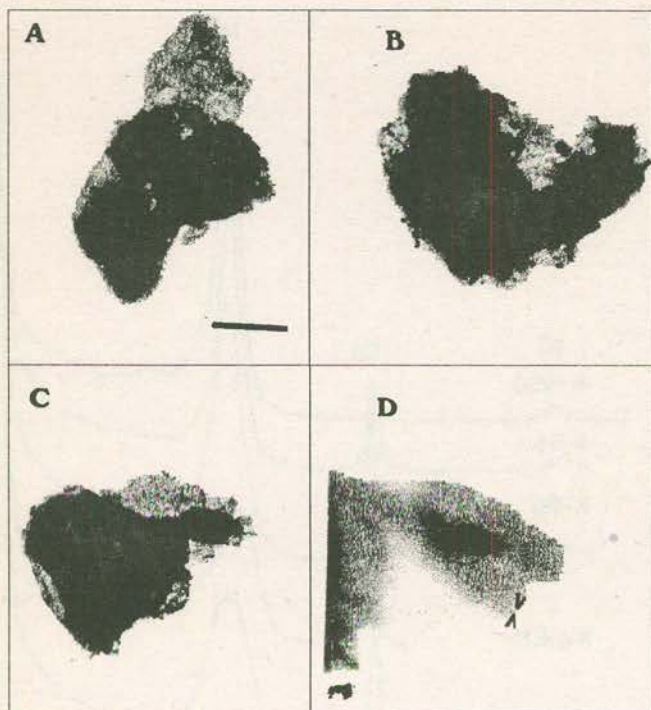
Fig 3..Transmission electron micrographs of the clay (<2 μm) size fraction: (A) sharp edged clay showing intergrowth of crystal, bar = 555 Å; (B) thin particle with frayed edges, opaque iron oxide spots, and diffused boundary, bar = 274 Å; (C) layered particle with frayed edges; and (D) high resolution electron micrograph of layered particle showing interlayer repeat distance of 10.1 Å.

Fig 4. Maize plant growth in nutrient solution medium.
-K, no potassium was added; +K, potassium at full dose; Glauc, 10g of glauconitic sandstone.

hours, kaolinite structure decomposed and consequently the 7.0 Å peak disappeared.

The clay particles were of variable morphology as observed with the TEM (Fig 3). Although, most particles were platy, only few particles had clean smooth edges (Fig 3A) while most had diffused boundary and porous structure (Fig 3B). Many particles showed signs of weathering and curling-up of individual layers (Fig 1E, Fig 3C). One particular clay particle and interlayer space repeat distance of 10.1 Å When seen at high resolution (Fig 3D). Some ferruginous contamination in the clay fraction was evident by the opaque spots on the clay particles (Fig 3B).

The clay contained 50% mica as indicated by the total K content and 4% vermiculite and 10% smectite as indicated by Ca/Mg and NH_4/K cation exchange capacity method (Table 1). The clay had 190 mmol Fe, 34 mmol Mg and 80 mmol K per 100g. The clay had higher Fe/Mg ratio than the reference glauconite.

Generally, a higher-temperature endothermic peak in the range of 1073 to 1273 Kelvin indicates the presence of well crystallized mica (muscovite, paragonite, biotite). Two endothermic peaks, one at about 423 to 513 Kelvin and other at 773 to 973 Kelvin, indicate the presence of poorly crystalline, K deficient mica (illite, glauconite). In this study the shoulder on low-temperature side of 873 and 513 Kelvin of DTA peaks (data not presented was attributed to glauconite. The broad peak around 873 to 893 kelvin represents dehydroxylation. The glauconite DTA were similar to those of illite (Fanning *et al* 1990).

Glauconite formation results primarily from authigenic crystal growth that begins from poorly crystallized Fe-rich smectite-like layer silicate. In a K rich geochemical environment, it quickly evolves into a better-crystallized glauconite phase (Odom 1984). As the precipitation proceeds, the glauconite-smectite phase transforms into disordered glauconite and then to ordered glauconite. In this case, the substrate appeared to be non-micaceous, porous matter. As, the sand grains are coated with re-precipitating substrate, it appeared that glauconite crystal growth occurred in the sand framework (Odin and Matter 1981). If assumed that the kaolinite is authigenic, presence of about 25% kaolinite may point towards the K-deficient geochemical environment at the end of the glauconite formation process.

Plant growth and K-uptake. The glauconitic sandstone maintained 0.1 ppm K concentration over the growth period in the nutrient solution (Table 2), which initially had no K. The solid phase maintained an equilibrium concentration 8 to 10 times less than the commonly found soil solution K-values (Tisdal *et al* 1985). Potassium concentration in the

tions as the sum of vermiculite + smectite (total expandable portion) was about 14%. Potassium saturation and heat treatment to 623 Kelvin and 823 Kelvin resulted in an enhanced sharp and symmetric 10 Å peak. There was no change in the kaolinite peak position or width except, when K-saturated sample was heat treated at 823 Kelvin for two

maize plant with glauconitic sandstone was half that of the plant grown on full K (Table 2). Similarly, dry weight of shoot and root of the plant with glauconite was half that of the plant grown on full K (Fig 4). Plant growth and K-uptake study suggested that the glauconitic sandstone may provide a slow but steady source of K for growing plants; however, further experimentation is needed to prove its suitability for field crops.

References

Bailey S W 1980 Structure of Layer Silicates. In: *Crystal Structure of Clay Minerals and their X-ray Indentification,* eds Brindley G W & Brown G. Mineralogical Soc, London, pp 1-125.

Baqri S R H, Hussain V, Bilqees R, Jan N, Ahmad N 1994 Petrographic and chemical characteristics of glauconitic and phosphatic sediments of the Kussak Formation, Khewra Gorge, Salt Range, Pakistan. *Pak J Sci Ind Res* **37** 291-296.

Birch Y K, Willis J B, Rickard R S 1976 An electron microprobe study of glauconite from the continental margin off the west cost of S. Africa. *Marine Geology* **22** 271-284.

Brindley G W 1980 Order-disorder in clay minerals structure. In: *Crystal Structure of Clay Minerals and their X-ray Identification,* eds Brindley G W & Brown G. Mineralogical Soc, London, pp 126-189.

Danilchik W, Shah S M I 1987 *Stratigraphy and Coal Resources of the Makarwal Area, Trans-Indus Mountains, Mianwali District, Pakistan.* U S Geological Survey Professional paper 1341. U S Govt. Printing Office, Washington.

Fanning D S, Keramidas V Z, El-Desoky M A 1989 Micas. In: *Minerals in Soil Environment,* eds Dixon J B & Weed S B. Soil Sci Soc Am Book Series No.1, Soil Sci Soc Am Wisconsin, USA, pp 551-634.

Fatmi A N 1972 Statigraphy of the Jurassic and Lower Cretaceous rocks and Jurassic ammonite from northern areas of West Pakistan. *British Mus Natural History Bull* **20** 300-381.

Inn R P, Pluth D J 1970 Thin-section preparation using an epoxy impregnation for petrographic and electron microproble analysis. *Soil Sci Soc Am J* **34** 483-485.

Jackson M L 1979 *Soil Chemical Analysis Advanced Course.* 2nd ed. Publ by the author, Dept Soil Sci, Univ. Wisconsin, Madison, Wisconsin pp 895.

Moore D M, Reynolds Jr R C 1989 *X-ray Diffraction and the Identification and Analysis of Clay Minerals.* Oxford University Press, New York pp 332.

Odom E 1984 Glauconite and celadonite minerals. In: *Micas. Review in Mineralogy,* ed Bailey S W. Mineralogical Soc. Am. Washington, DC USA, Vol 13.

Thompson G R, Hower J 1975 Mineralogy of glauconite. *Clays Clay Minerals* **23** 289-300.

Tisdal S L, Nelson W L, Beaton J D 1985 Soil Fertility and Fertilizers. Macmillan Publ Co, New York, 4th ed, pp250.